Supplementary Information (SI) for Nanoscale.


*Supplementary Material*

# Interplay between superconducting fluctuations and weak localization in disordered TiN thin films

*Sachin Yadav,[1,2] Bikash Gajar,[1,2] R. P. Aloysius,[1,2] and Sangeeta Sahoo[1,2,*]*

*[1]CSIR-National Physical Laboratory, Dr. KS Krishnan Marg, New Delhi-110012, India*

*[2]Academy of Scientific and Innovative Research (AcSIR), Ghaziabad- 201002, India*

**Correspondences should be addressed to S. S. (Email: sahoos@nplindia.org)*

***Contents:***

**1. Calculation of Ginzburg- Landau (GL) coherence length ($\xi_{GL}$) for TiN sample**

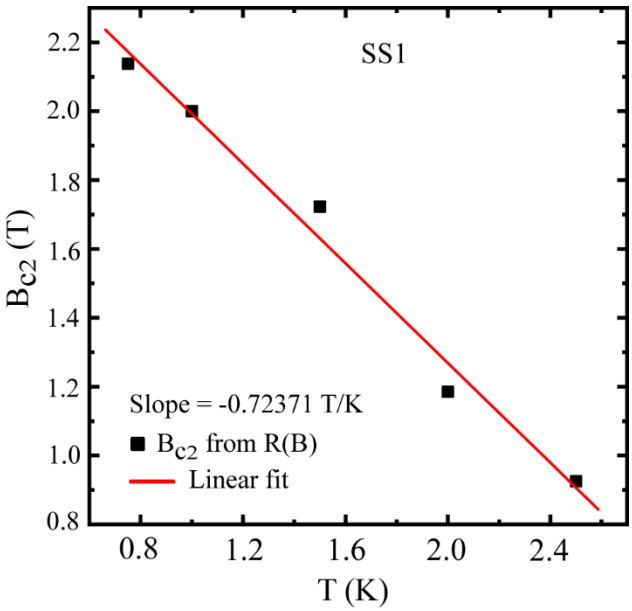


***Fig. S1:*** *B-T phase diagram for the TiN sample SS1. Black squares are the data points collected from R(B) isotherms and the solid red line represents the linear fit to the experimental points which provides the slope for calculating the Ginzburg-Landau (GL) coherence length* $\xi_{GL}$.

The Ginzburg-Landau (GL) coherence length $\xi_{GL}(0)$ for sample SS1 is calculated by using the formula, $\xi_{GL}(0) = \left[\frac{\phi_0}{2\pi T_c \left|\frac{dB_{c2}}{dT}\right|_{T_c}}\right]^{1/2}$, where $\phi_0$ is the flux quantum. The experimental data points are collected from the upper critical field ($B_{c2}$) values from respective *R(B)* isotherms. The extracted values from *R(B)* are fitted linearly in Fig. S1 as shown by the red line. The slope obtained from the linear fit has been used for calculating the coherence length $\xi_{GL}(0)$ for the TiN sample with $T_c$ = 2.45 K and the obtained coherence length is about ~ 9 nm.

**2. Quantum corrections to the conductivity (QCC) fit along with its individual components:**

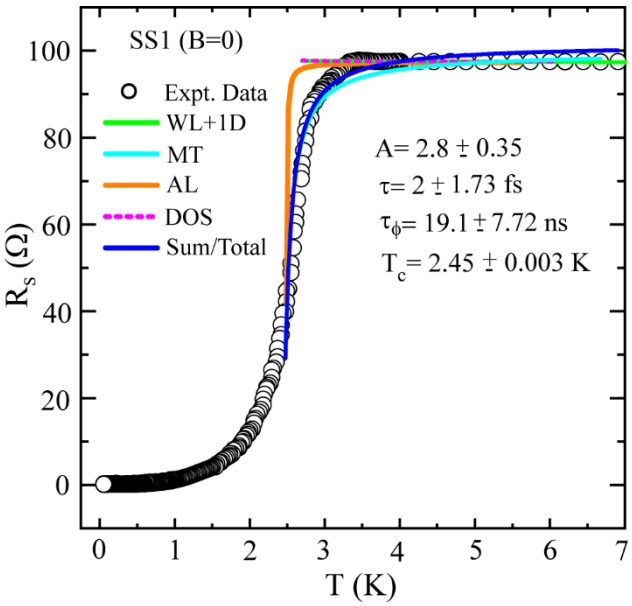


***Fig. S2:*** *QCC fits to zero-field R(T) data for sample SS1 using Equations (3)-(7) from the main article that show the fits related to the individual quantum contributions and also the sum of all the contributions. Here, $T_c$ =2.45 K, obtained from MT fit.*

### 3. Halperin-Nelson fit to zero field $R_S(T)$ curve to confirm the 2D nature:

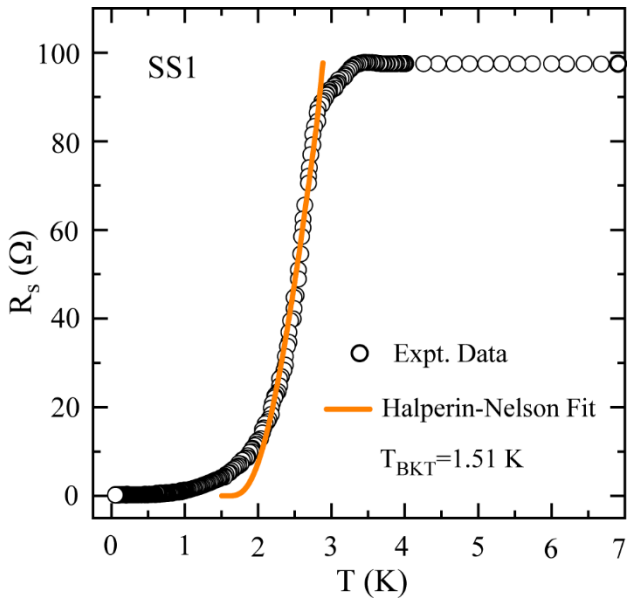


***Fig. S3:*** *Zero field $R_S(T)$ curve of the sample SS1. The solid orange curve represent the Halperin-Nelson fit [Equation (1)], where $T_{BKT}$ is obtained at 1.51 K.*

The experimental $R_S(T)$ is fitted with Halperin-Nelson (HN) formula (the orange solid curve) and given by expression, [1]

$$R_S(T) = R_0 exp\left[-b/(T - T_{BKT})^{1/2}\right], \qquad (1)$$

where, $T_{BKT}$ is the BKT transition temperature and $R_0$ and $b$ are constants. The values of the constants $R_0$ and $b$ from the fit are 4326 and 4.49, respectively and the $T_{BKT}$ = 1.51 K. However, the deviation from the experimental data at low temperature indicates that the BKT transition is suppressed at low temperature. The deviation originates from finite size effects and inhomogeneity [2,3] or it could be due to macroscopic quantum tunneling. [1]

**4. Correlation of $\delta R_S$ with the zero field $R_S(T)$ for the sample SS1:**

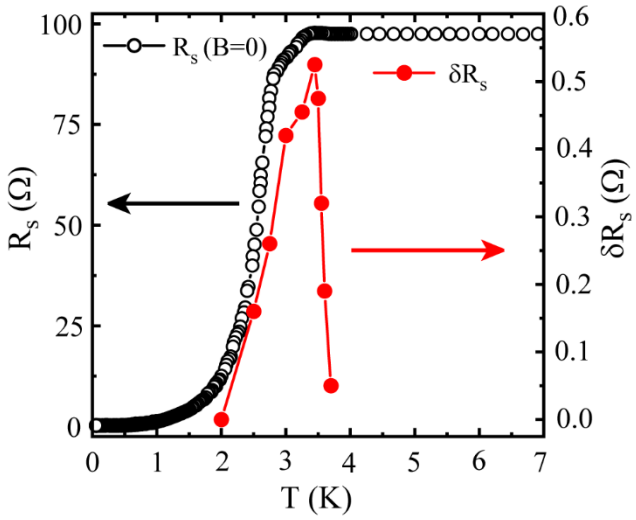


***Fig. S4:*** *Comparison of $\delta R_S$ with respect to the zero-field $R_S(T)$*

**5. Zero-field *R(T)* and *R(B,T)* data for sample SS3:**

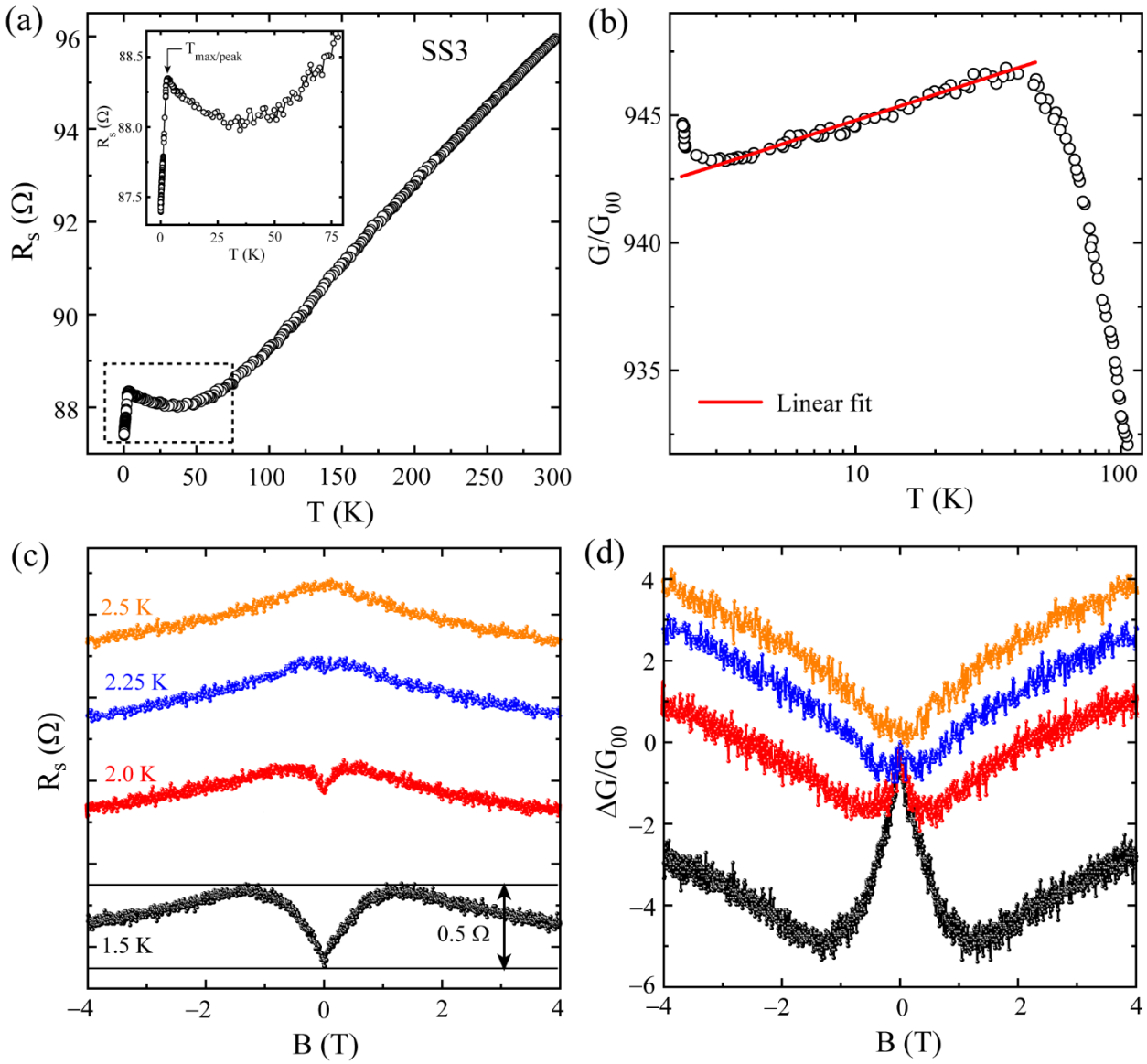


***Fig. S5:*** *Zero-field R(T) & R(B,T) measurements for sample SS3. (a) Zero-field R(T) data measured from room temperature (300 K) down to 1 K. The region marked by the black dotted rectangle is highlighted in the inset which shows a resistance minimum/dip followed by a resistance maximum/peak before transiting to the superconducting state while cooling down the sample. The deviation from normal metallic behavior is evident by the prersence of the upturn in the R(T) which generally occurs due to electron elctron interaction and/or weak localization in disordered superconductors. The temperature $T_{max/peak}$ corresponding to the resistance peak/maximum is marked by the arrow in the inset of (a). (b) The logarithmic temeperature dependence of R(T) in terms of dimenisonless conductance. The red line is the linear fit to the experimental data in log(T) scale. (c) A set of selective R(B) isotherms measured at different temperatures for sample SS3. The R(B) isotherms are shifted vertically for clarity to show a crossover from positive to negative magnetoresistance as T increases towards $T_{max/peak}$. (d) The corresponding magnetoconductance in unit of dimenisonless conductance showing the evolution of MC curves with temperature.*

## 6. Comparison between MC fittings between with and without extra coefficients for WL & MT terms:

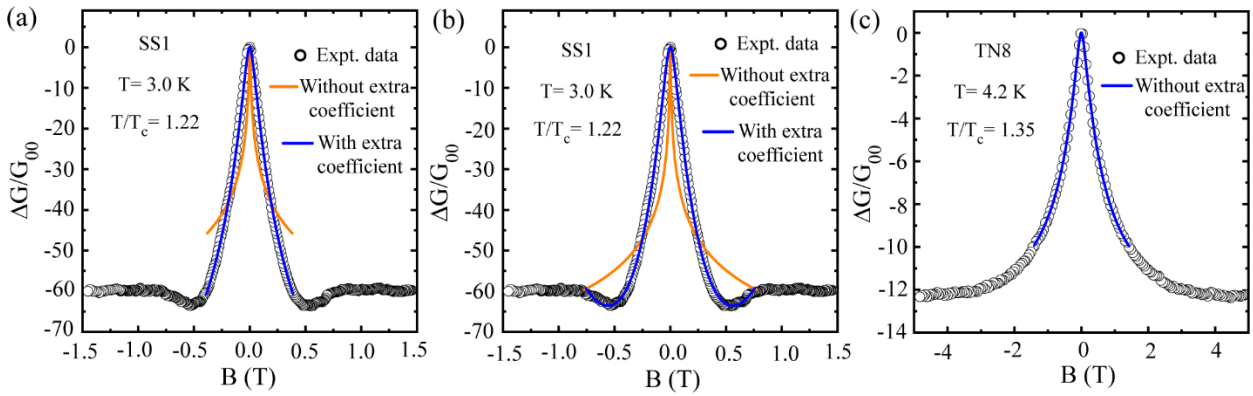


***Fig. S6:*** *Quantum corrections (SF+WL) to magnetoconductivity fits with (the blue solid curve) & without (the orange curve) extra coefficients attached to MT and WL terms for sample SS1 (a) in the low field range covering only negative MC region and (b)in the high field range containing both negative and positive MC regions. (c) The quantum corrections to magnetoconductivity fit with no extra coefficient for another sample TN8 with higher normal state resistance and with mostly negative MC. The open circles represent experimental data and the solid curves act for the fits.*

## 7. Thickness measurement by AFM:

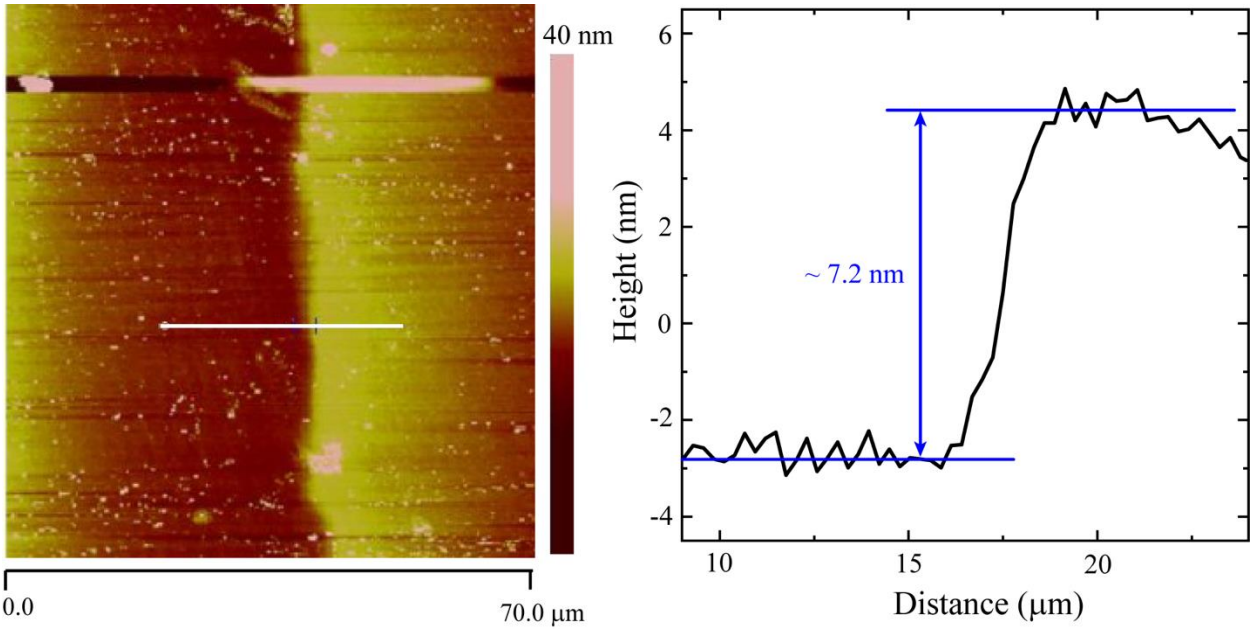


***Fig.S7:*** *(Left) AFM image of the TiN thin film sample (SS1) (after the nitridation) and (Right) the corresponding film thickness is estimated by height profile analysis.*

## 8. Collection of TiN samples having different growth conditions:

We have carried out similar measurements on many other samples that show resistance upturn in their zero-field *R(T)* characteristics and the sample details are collected in Table S1. We observe that the upturn and the related zero-field resistance peak lead to negative magnetoresistance at the peak temperature ($T_{max}$) for the samples with normal state square resistance in the range of 85-100 Ω and the thickness in the range of 5-8 nm. On the contrary, positive magnetoresistance is observed at the same temperature $T_{max}$, corresponding to the peak temperature in zero-field *R(T)* measurements, for the samples with higher square resistance. The second set of higher resistive samples undergo magnetic field induced SIT at higher field (data not shown here).

**Table S1:** Parameters of the TiN films measured in the course of the present study. $R_{Max}$ and $R_N^{300K}$ are in resistance per square. $T_a$ is the annealing temperature for the growth. $T_{max}$ is the temperature corresponding to the resistance peak appears in zero-field *R(T)*. *d* corresponds to the thickness of the films. D denotes the diffusion constant for all the TiN samples.

| ***Samples*** | ***$T_a$ (℃) ± 10℃*** | ***Pressure during annealing (Torr)*** | ***d (nm)*** | ***$T_C$ (K) (from QCC fit)*** | ***D, ($cm^2 s^{-1}$)*** | ***$R_{Max}$ (Ω)*** | ***$R_N^{300K}$ (Ω)*** | ***Type of MR at $T_{max}$*** |
|---|---|---|---|---|---|---|---|---|
| SS1 | 750 | $1.8 \times 10^{-7}$ | 7 ± 1 | 2.45 | 0.810 | 98 | --- | ***Negative*** |
| SS2 | 750 | $1.3 \times 10^{-7}$ | 6 ± 1 | 2.0[a] | 0.724 | 86 | 101 | |
| SS3 | 730 | $1.5 \times 10^{-7}$ | 8 ± 1 | 2.85[a] | --- | 88 | 96 | |
| TN3 | 820 | $4.8 \times 10^{-8}$ | 8 ± 1 | 4.3 | --- | 70 | 97 | ***Positive*** |
| TN4 | 820 | $4.7 \times 10^{-8}$ | 4 ± 0.8 | 3.55 | 0.612 | 150 | 186 | |
| TN5 | 820 | $4.6 \times 10^{-8}$ | 3 ± 0.5 | 2.93 | 0.405 | 352 | 400 | |
| TN8 | 780 | $2.2 \times 10^{-8}$ | 4 ± 0.8 | 3.1 | 0.589 | 139 | 168 | |
| TN9 | 780 | $2.1 \times 10^{-8}$ | 3 ± 0.5 | 2.43 | 0.429 | 332 | 367 | |
| TN10 | 780 | $1.7 \times 10^{-8}$ | 2 ± 0.5 | 1.93 | 0.245 | 1246 | 1227 | |
| TN12 | 750 | $1.3 \times 10^{-8}$ | 4 ± 0.8 | 2.47 | 0.567 | 148 | 174 | |
| TN13 | 750 | $1.2 \times 10^{-8}$ | 3 ± 0.5 | 2.35 | 0.405 | 349 | 386 | |

[a] $T_c$ onset values are considered.

**References:**

[1] Y.-H. Lin, J. Nelson, A.M. Goldman, Physical Review Letters 109 (2012) 017002.

[2] T. Schneider, S. Weyeneth, Physical Review B 90 (2014) 064501.

[3] L. Benfatto, C. Castellani, T. Giamarchi, Physical Review B 80 (2009) 214506.